Metamagnetic transition in $Ce(Fe_{0.96}Al_{0.04})_2$: a dc magnetization study

2002 J. Phys.: Condens. Matter 14 4477

(http://iopscience.iop.org/0953-8984/14/17/318)

INSTITUTE OF PHYSICS PUBLISHING JOURNAL OF PHYSICS: CONDENSED MATTER

J. Phys.: Condens. Matter **14** (2002) 4477–4490 PII: S0953-8984(02)25109-7

Metamagnetic transition in $Ce(Fe_{0.96}Al_{0.04})_2$: a dc magnetization study

Meghmalhar Manekar, Sujeet Chaudhary, M K Chattopadhyay, Kanwal Jeet Singh, S B Roy and P Chaddah

Low Temperature Physics Laboratory, Centre for Advanced Technology, Indore 452013, India

Received 16 May 2001, in final form 1 March 2002
Published 18 April 2002
Online at stacks.iop.org/JPhysCM/14/4477

Abstract

We present results of a dc magnetization study which show interesting thermomagnetic history effects across the antiferromagnetic-to-ferromagnetic transition in $Ce(Fe_{0.96}Al_{0.04})_2$ pseudobinary alloy. Specifically, we observe (i) the degree of ZFC/FC irreversibility rising with increasing field; (ii) the virgin curve lying outside the envelope M–H curve. Some of the key results are supported by magneto-transport measurements. We argue that these effects are quite different from the characteristics seen in spin glasses or in hard ferromagnets. They can be understood in terms of kinetic arrest of a first-order transition.

1. introduction

The C15 Laves phase compound $CeFe_2$ has an anomalously low T_C ($\approx$235 K) and saturation magnetic moment ($\approx$2.3 μ_B/f.u.) [1, 2] compared to the other RFe_2 (R = rare-earth metals) series compounds. Neutron scattering has shown the presence of antiferromagnetic (AFM) fluctuations in this ferromagnetic (FM) compound [3] indicating that it is on the verge of a magnetic instability. This instability can be triggered by doping with certain elements such as Al, Ir, Ru, Re, Os and Co on the Fe site [4–10] causing a FM-to-stable-AFM transition, whereas replacement of Fe by Ni, Mn, Rh, Pd only has the effect of diluting the ferromagnetism [5, 7] indicating that the transition is driven by the change in electronic structure and not driven by impurities. It was predicted by Eriksson *et al* [2] that the Ce orbital 4f moment is almost quenched and the magnetic moment on the Ce atom is antiparallel to the moment on the Fe atom. These predictions were later verified by means of polarized neutron diffraction [11], magnetic circular x-ray dichroism (MCXD) [12–14] and magnetic Compton scattering [15]. These experiments exhibited substantial discrepancies as regards the values of the Ce moment found, but conclusively showed that the Ce moment is aligned antiparallel to the Fe moment. Furthermore, it was shown by MCXD experiments that substitution of Co at the Fe site does not affect the Ce moment [12]. Therefore the FM–AFM transition upon certain dopings seems to arise from the instability in the Fe sublattice and not due to the change in the magnetic state of the

Ce sublattice. These results along with the recent magnetization and transport measurements on $(Ce_ySc_{1-y})Fe_2$ [16] show the importance of the nature of hybridization between the Ce 4f and Fe 3d electrons in understanding the magnetic properties of $CeFe_2$-based systems.

While the above-mentioned efforts were directed more towards understanding the cause of the magnetic instability, some efforts have also been made to achieve an understanding of the nature of the FM-to-AFM phase transition. It is conjectured that the FM-to-AFM transition in $Ce(Fe_{1-x}Co_x)_2$ [17, 18] accompanied by a cubic-to-rhombohedral distortion [19] of the lattice is first order in nature. We have recently shown that the transition from FM to AFM in Ru- and Ir-doped $CeFe_2$ is also a first-order transition [20].

In the present paper we focus our attention on the FM-to-AFM transition in $Ce(Fe_{0.96}Al_{0.04})_2$. This system is particularly interesting as it shows a broad FM-to-AFM transition as compared to the Ru- and Co-doped samples [19]. The cause of the dependence of the width of transition on the type of dopant is not very clear at the moment, but it has been speculated that it may be a local perturbing potential at the Fe site (which would depend upon the type of dopant) causing a gradual (or sharp) reorientation of the magnetic moments [21] during the transition. In our earlier work [20] on Ru- and Ir-doped $CeFe_2$, we have emphasized the first-order nature of the FM–AFM transition by highlighting the presence of hysteresis and phase coexistence in both the temperature and field cycles. The FM–AFM transition in both the samples is quite sharp and the width of hysteresis is quite narrow, thus providing us with a narrow temperature and field regime in which to study various thermomagnetic history effects across the transition. The transition in Al-doped $CeFe_2$—being much broader and having a wider phase coexistence regime [19] in comparison to the Ru- and Ir-doped $CeFe_2$—offers us a much better opportunity to study various thermomagnetic history effects across the transition. We thus expect that all the features that we observed in the Ru- and Ir-doped $CeFe_2$ should show up more prominently in the Al-doped sample under consideration in the present work.

2. Experimental procedure

The sample used in the present study belongs to the same batch of samples as were used earlier in the study of bulk magnetic and transport properties [6] and neutron measurements [19]. The details of sample preparation and characterization can be found in [6]. We have used a commercial SQUID magnetometer (Quantum Design-MPMS5) for measuring magnetization (M) as a function of temperature (T) and magnetic field (H). We have checked the results by varying the scan length from 2 to 4 cm and no qualitative dependence on the scan length is found. The sample chamber was flushed with helium gas at 200 K before each experimental cycle. This was done to get rid of any residual oxygen leaking into the sample chamber over a period of time. A commercial superconducting magnet and cryostat system (Oxford Instruments UK) was used for magneto-transport measurements as a function of T and H. The resistivity ρ was measured using a standard dc four-probe technique.

3. Results and discussion

3.1. Metamagnetic transition and phase coexistence

Figure 1 shows a zero-field-cooled (ZFC) M–H curve at $T = 80$ K with the ZFC M–H curve at $T = 100$ K as an inset. In the ZFC protocol, the sample is cooled in zero field from a temperature above T_C to the temperature at which the measurement is done and then the measuring field is switched *on*. From figure 1 of [6] it is apparent that FM order exists for $T \geqslant 100$ K. The M–H curve at 100 K is that of a conventional ferromagnet reaching technical

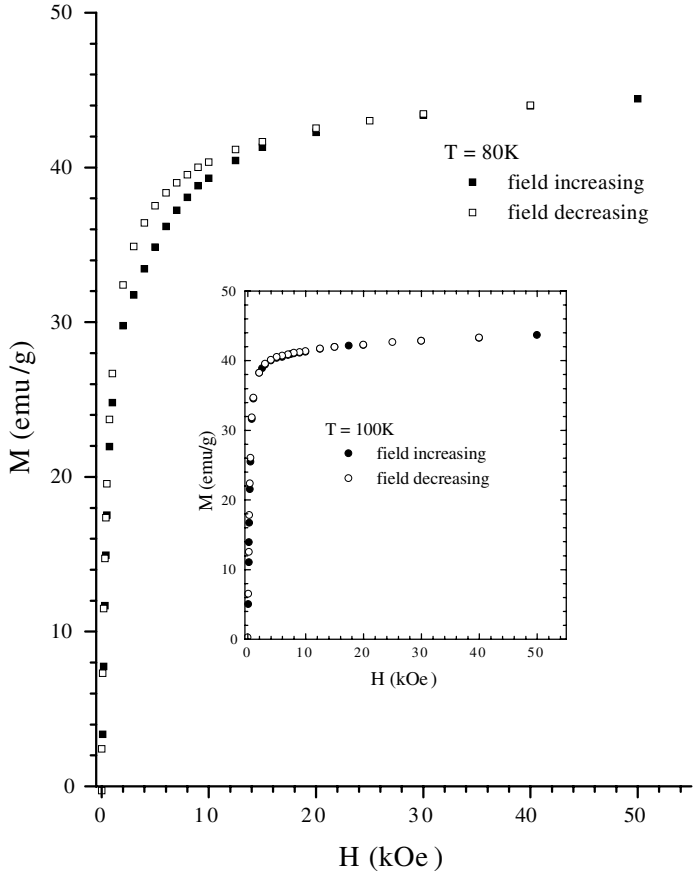

Figure 1. The magnetization versus field plot at $T = 80$ K. The inset shows the magnetization versus field plot for $T = 100$ K. The measurements are done in the ZFC mode.

saturation by $H \approx 3$ kOe and having a coercive field of roughly 100 Oe. The nature of the M–H curve changes drastically as the temperature is lowered and at 80 K a distinct hysteresis bubble opens up with a fairly reversible field regime before and after the bubble. Very similar M–H curves were obtained in our earlier study on Ir- and Ru-doped $CeFe_2$ samples [20]. As we further lower the temperature, this hysteresis bubble opens up further.

The ZFC M–H curve obtained at $T = 5$ K is shown in figure 2. The magnetization shows a sharp rise at $H \approx 30$ kOe indicating a field-induced FM transition. We define the onset field of the AFM–FM transition as H_M. H_M is estimated as the field at which the M–H curve changes curvature from convex to concave. Below this field the sample is in the AFM state. The non-linearity at low fields ($H \leqslant 5$ kOe) is probably due to a parasitic ferromagnetism [22] leading to a spin canted state [19]. We will discuss this non-linear behaviour in detail later. When the field is reduced after crossing the critical value H_M, a large hysteresis is observed. A sharp rise in magnetization accompanied by hysteresis is traditionally taken as a signature of a first-order magnetic transition [23, 24]. This hysteresis is different compared to a hysteresis in hard ferromagnets arising due to domain wall pinning and/or anisotropy in the sense that the hysteresis in the case of a ferromagnet has its maximum width at $H = 0$, whereas in our case the width of the hysteresis almost goes to zero at $H = 0$. The hysteresis observed at 5 K

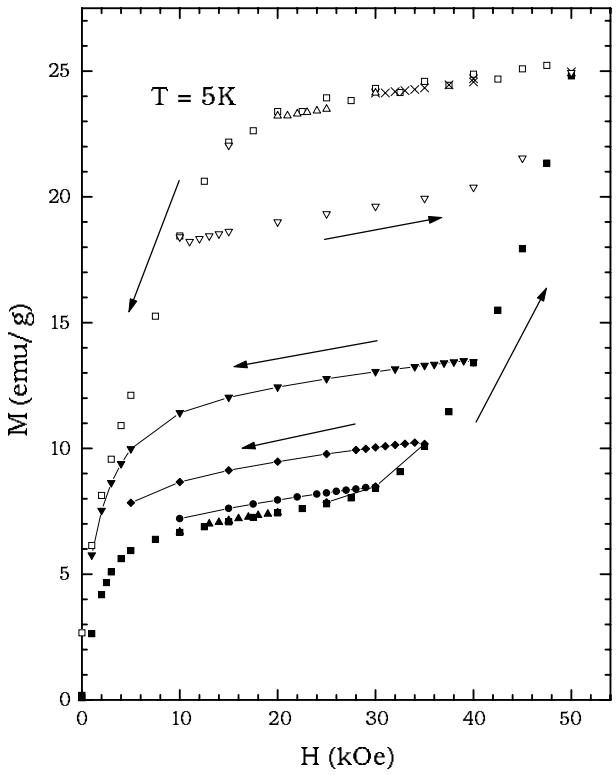

Figure 2. MHLs initiated during both the ascending-field cycle and the descending-field cycle at $T = 5$ K. MHLs initiated during the ascending-field cycle at $H = 20$ kOe (solid upward-pointing triangles), $H = 30$ kOe (solid circles), $H = 35$ kOe (solid diamonds), $H = 40$ kOe (solid downward-pointing triangles) and during descending-field cycle at $H = 30$ kOe (crosses), $H = 20$ kOe (open upward-pointing triangles) and $H = 10$ kOe (open downward-pointing triangles). The virgin curve and the envelope curve are shown by solid squares and open squares respectively. The lines are guides to the eye.

cannot arise due to the intrinsic property of the field-induced FM state as we now show. We first assume that the hysteresis shown in figure 2 is due to the intrinsic nature of the field-induced FM state with the entire M–H loop shifted away from the origin. In that case the width of the hysteresis (almost 30 kOe) cannot be explained as compared to the coercivity field (about 100 Oe) when the sample is in the FM state (see figure 1).

An observation showing more conclusively that the hysteresis is not due to domain wall pinning and/or anisotropy comes from our magneto-transport measurements on the same sample (see the inset of figure 4(a)). The transport mean free path is usually much smaller than the typical dimensions of the domain walls and hence there should be a negligible contribution of scattering from domain walls to the features observed in transport properties.

Apart from hysteresis, the other signature of a first-order transition is a phase coexistence. The first qualitative indication of phase coexistence comes from the nature of the M–H curve. At $T = 5$ K, the M–H curve at field values above H_M ($\approx$30 kOe) has a smaller slope compared to the initial slope of the M–H curve at 100 K where the entire sample is in the FM state. This indicates that the AFM–FM transition takes place over a broad field regime and both these phases coexist along the M–H curve at field values above H_M. We now show the experimental

observation of phase coexistence through the technique of minor hysteresis loops (MHLs) [20]. A MHL results when the direction of the change of field is reversed before the transition is completed. One can initiate a minor loop on the ascending-field cycle (i.e. reduce the field before the transition is completed) and also on the descending-field cycle (i.e. increase the field before the transition is completed). The minor loop initiated at a 'low enough' field (20 kOe) in the field-increasing cycle on the virgin curve is completely reversible, indicating that the transition has not yet begun (see figure 2). As we initiate minor loops from higher fields we start observing hysteresis and the amount of hysteresis increases as the value of the field of initiation of the MHL is increased. This indicates that the field-increasing curve (above H_M) corresponds to the AFM phase transforming to a FM phase with the AFM phase persisting as a metastable phase over some field regime. Similarly the field-decreasing curve (50–0 kOe) corresponds to the FM phase transforming to an AFM phase with the FM phase persisting as a metastable phase over some field regime. Further evidence of supercooling comes from the nature of the MHL initiated in the descending-field cycle at $H = 10$ kOe (see figure 2). At $H = 10$ kOe during the ascending-field cycle the entire sample is in an AFM phase as discussed earlier, whereas most of the sample is in a FM state at the same field value during the field-decreasing cycle. The MHLs thus show the presence of phase coexistence in the region bounded by the envelope curve. Had there been no phase coexistence we would not have been able to produce any MHL and all the minor loops would have been reversible. Similar MHLs have been obtained at $T = 50$ K and are presented in figure 3.

Having established the first-order nature of the field-induced transition we now focus our attention on certain unusual features of the M–H and ρ–H curves.

3.2. Anomalous features in isothermal field dependence of magnetization

The hysteresis loop collapses before $H = 0$ and reappears in the third quadrant when the field crosses H_M in the negative direction, resulting in a *butterfly loop* (see figure 4(*a*)). Such double loops have been observed in ferroelectrics and it has been conclusively shown that only a first-order transition can explain this feature [25]. We are unaware of similar arguments in the case of AFM-to-FM transition. In our present material, on reversing the direction of the field through zero we find an anomalous situation where the virgin curve lies outside the envelope curve. (The virgin curve in the negative direction is obtained by ZF cooling the sample and then increasing the field in the negative direction.) This anomalous behaviour of the envelope curve lying above the virgin curve remains on reversing the field through zero in the positive direction. Similar behaviour is observed in our magneto-transport studies on the same sample. The virgin resistivity (ρ) versus field curve lies outside the envelope ρ–H curve (see the inset of figure 4(*a*)). Figures 4(*b*) and (*c*) show a similar anomalous relation between the virgin and the envelope M–H and ρ–H curve respectively at higher temperatures. Such a relation between the virgin curve and the envelope curve is quite uncommon in magnetic materials except for some granular materials [26] where the surface-to-volume ratio plays an important role and in iron–cobalt–nickel alloys [27]. In the case of the Fe–Co–Ni alloys we are not aware of an explanation for such a anomalous relation between the virgin and envelope curve. In our bulk material the surface-to-volume ratio is definitely much smaller than was the case in [26] and also the magnetic property of our material is different from those of Fe–Co–Ni alloys. To the best of our knowledge, this is the first time that a virgin curve has been reported to lie outside the envelope curve during a first-order AFM–FM transition. After the first field cycling the virgin state is lost and we are not able to get back the stable AFM state.

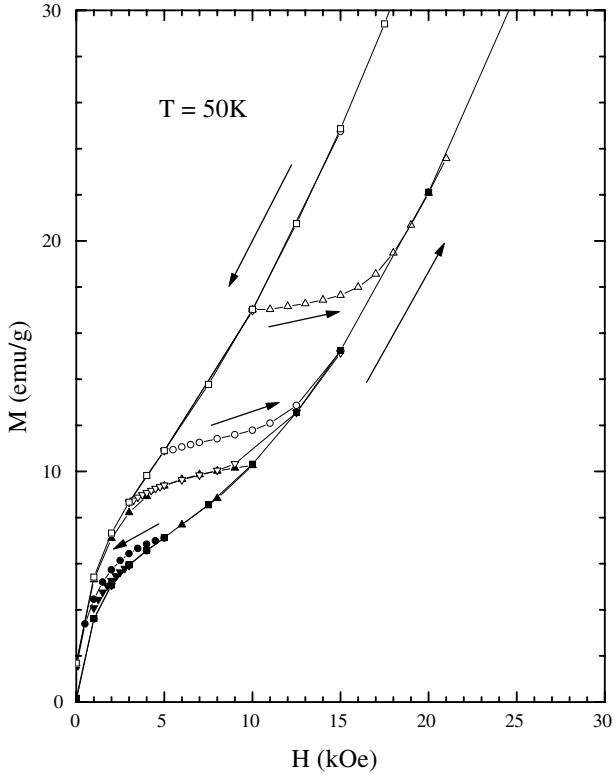

Figure 3. MHLs at $T = 50$ K. MHLs initiated during the ascending-field cycle at $H = 3$ kOe (solid downward-pointing triangles), $H = 5$ kOe (solid circles), $H = 10$ kOe (solid upward-pointing triangles) and during the descending-field cycle at $H = 10$ kOe (open upward-pointing triangles), $H = 5$ kOe (open circles), $H = 3$ kOe (open downward-pointing triangles). The virgin curve and the envelope curve are shown by solid squares and open squares respectively. The lines are guides to the eye.

3.3. Magnetization versus temperature

In figure 5 we present M versus T curves, obtained both in the ZFC and field-cooled (FC) mode, at various applied fields H. In the FC mode, the sample is cooled in the presence of a field from a temperature above T_C down to the lowest temperature. The data in figure 5 were taken with increasing temperature in both the ZFC and FC modes (see the figure caption for the values of the fields at which these measurements are done). A sharp rise in M as a function of decreasing T indicates the transition from the paramagnetic (PM) to the FM state. This is followed by a sharp drop in M at a lower T indicating the onset of the FM–AFM transition. The PM-to-FM transition temperature ($T_C \approx 200$ K) and FM-to-AFM transition temperature ($T_N \approx 95$ K) obtained from the low-field (20 Oe) M–T curve (see figure 5(a)) agree well with those obtained earlier from ac susceptibility measurements [6]. The zero-field ρ–T data are shown as an inset to figure 5(a) where the PM-to-FM transition shows up as a change of slope in resistivity whereas the FM–AFM transition is indicated by a sharp increase in resistivity [28]. With the increase in H there is a marked decrease in T_N. A distinct thermomagnetic irreversibility (TMI; i.e. $M_{ZFC} \neq M_{FC}$) is observed in the M–T curves for 20, 50 and 100 Oe (see figure 5(a)) starting well inside the FM regime. This kind of TMI is

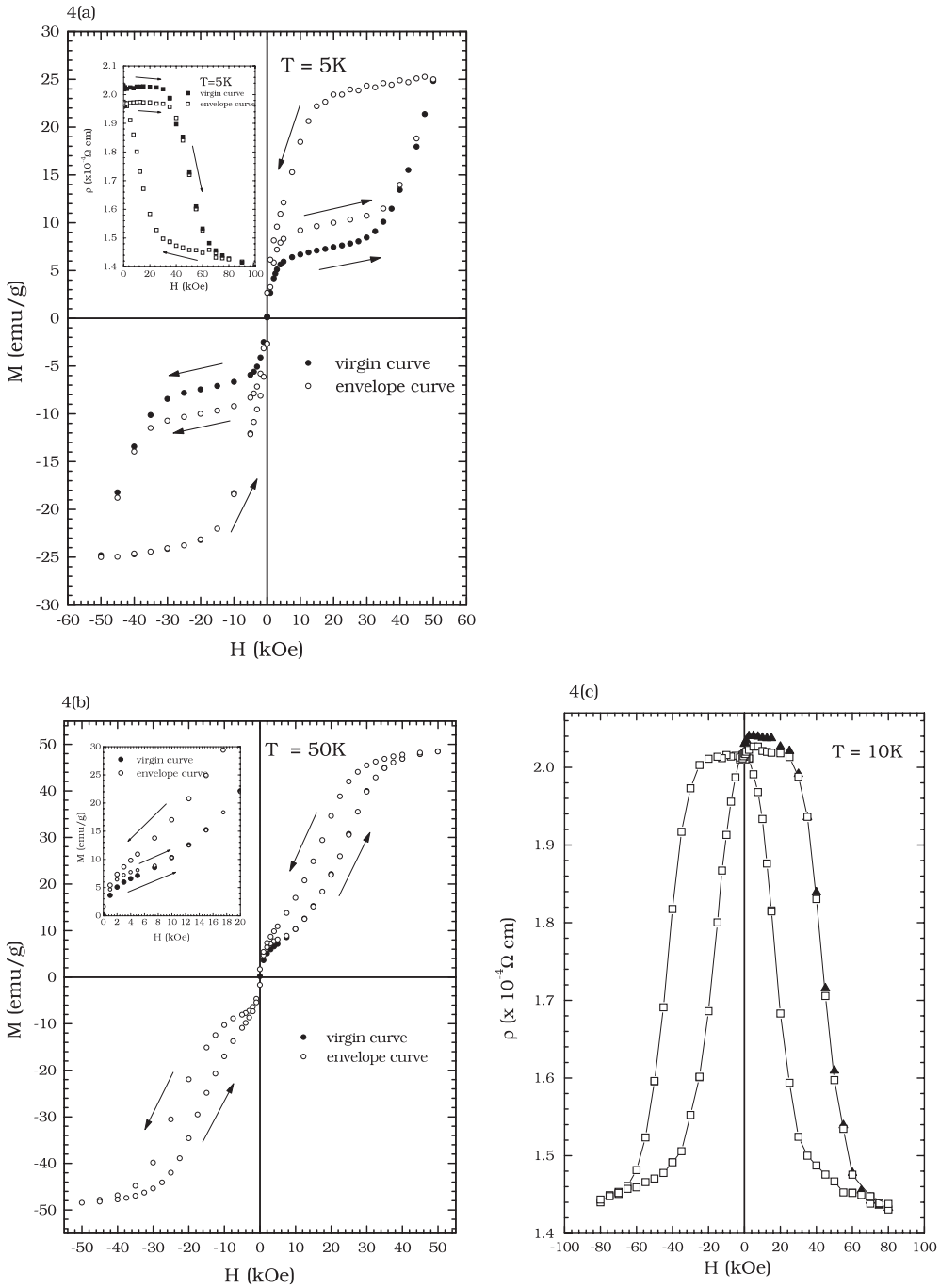

Figure 4. (*a*) The magnetization versus field *butterfly loop* at $T = 5$ K. The inset shows the ρ–H curve at $T = 5$ K. (see [35].) (*b*) The magnetization versus field *butterfly loop* at $T = 50$ K. The inset shows an expanded view. (*c*) The resistivity versus field curve at $T = 10$ K. Virgin curve: solid upward-pointing triangles; envelope curve: open squares. The curves are guides to the eye.

usually associated with spin-glass transition [29], but can also occur in a ferromagnet if the measuring field is of the order of the coercivity field [30]. With the measured coercivity of our sample in the FM regime being about 100 Oe, we attribute the observed TMI for $H \leqslant 100$ Oe to the residual domain-related pinning effects. In consonance with this conjecture, the TMI in the FM regime vanishes with further increase in H (see figures 5(a) and (b)).

While the TMI in the FM region vanishes for $H > 100$ Oe, a distinct TMI emerges in the AFM region. In contrast to the TMI in the FM region, this increases in strength with increasing H (see figures 5(a) and (b)). This is anomalous in comparison with the TMI associated with non-ergodic behaviour of the spin response in spin glasses and hindrance of domain rotation and/or domain wall pinning in ferromagnets. In both these cases the TMI is known to reduce with increase in the applied field.

In figure 6(a) we show the results on the M–T curve obtained during ZFC warming, field-cooled warming (FCW) and field-cooled cooling (FCC) for $H = 20$ kOe. At lower temperatures there is a distinct TMI in the ZFC and FCW curves. The FCW curve shows a minimum before merging with the ZFC curve at around $T = 55$ K. On FC cooling from temperatures well inside the reversible regime we get a distinctly different curve compared to the FCW curve. The FCC curve does not merge with the ZFC curve. We thus find that the ZFC state is lost in the first temperature cycle. In our SQUID magnetometer (Quantum Design-MPMS5) we do not have the facility to monitor the temperature lag between the sample and sensor and also cannot very efficiently cool the sample unidirectionally. We have done similar measurements on the same sample in our magneto-transport studies where our temperature control is much better and found qualitatively similar results for ρ versus T. Figure 6(b) shows the results of ρ–T measurements done in the ZFC, FCC and FCW modes at a field of 15 kOe. We thus believe that the observed features in M–T just mentioned are not related to any experimental artifact.

It is not necessary to field cool the sample from a temperature above T_N to observe the ZFC state getting erased. One can start cooling from the ZFC curve before reaching T_N and observe a similar kind of history effect. In figure 6(c) we show the result of one such experiment for $H = 30$ kOe. Here the temperature is first reduced from $T = 30$ K on the ZFC warming curve to 5 K and then the temperature is increased until the magnetization attains a value equal to that of the ZFC curve. The same procedure is repeated at $T = 40$ K. Similar results exist for thermomagnetic history effects in hard type-II superconductors [31] and for the case of hard ferromagnets as well [32].

To summarize the results of the M–H, ρ–H, ρ–T and M–T experiments, we say that the main observations are

(i) there is a hysteresis and phase coexistence across the field-induced AFM–FM transition;
(ii) the virgin curve lies outside the envelope M–H curve and is lost during the first field cycle; this feature in seen in the ρ–H curve as well;
(iii) the TMI in the M–T curves increases with increase in applied field, unlike the TMI seen in spin glasses and hard ferromagnets; and,
(iv) there is a distinct difference between the FCC and FCW M–T and ρ–T curves.

We now try to explain the anomalous results (ii), (iii) and (iv) in the following subsection.

3.4. Possible origin of anomalous features

We believe that the causes of the virgin curve lying outside the envelope M–H and ρ–H curves and the TMI increasing with the increase in field are the same.

In the M–T experiment, while cooling from the FM state to the AFM state, the FM state will continue to exist as a supercooled metastable state below T_N down to a certain

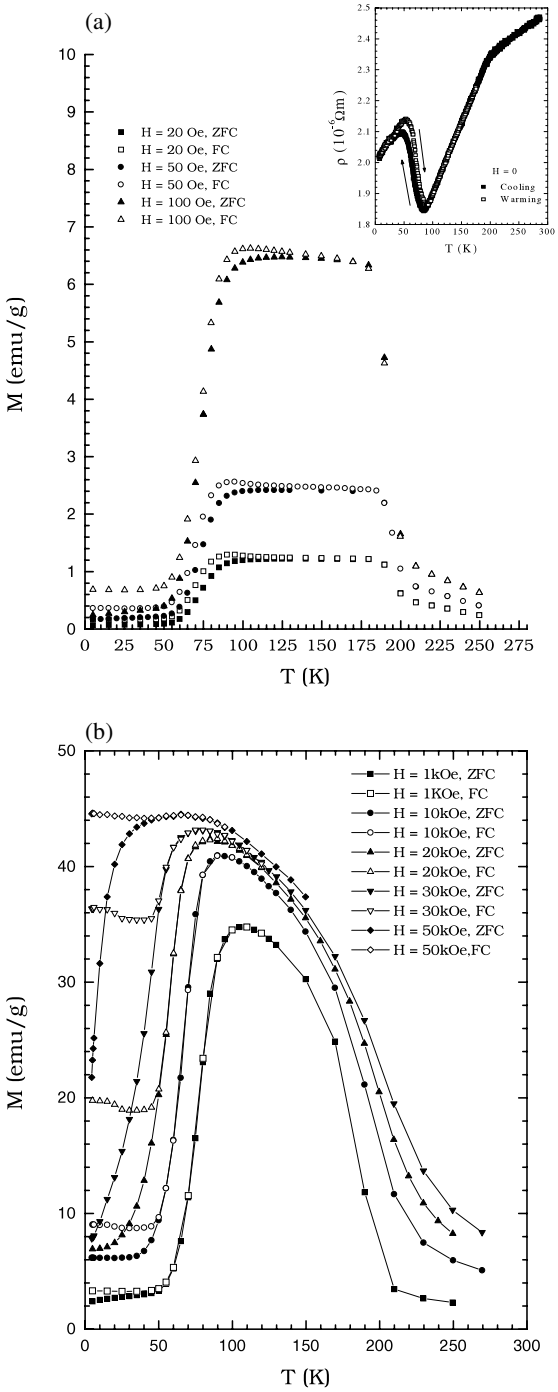

Figure 5. Magnetization versus temperature plots in ZFC and FC modes for various fields. The measurements are done with increasing temperature. In (*a*) the measurements are done at $H = 20$, 50 and 100 Oe. The zero-field resistivity as a function of temperature is shown as an inset (see [28]). In (*b*) the measurements are done at $H = 1$, 10, 20, 30 and 50 kOe.

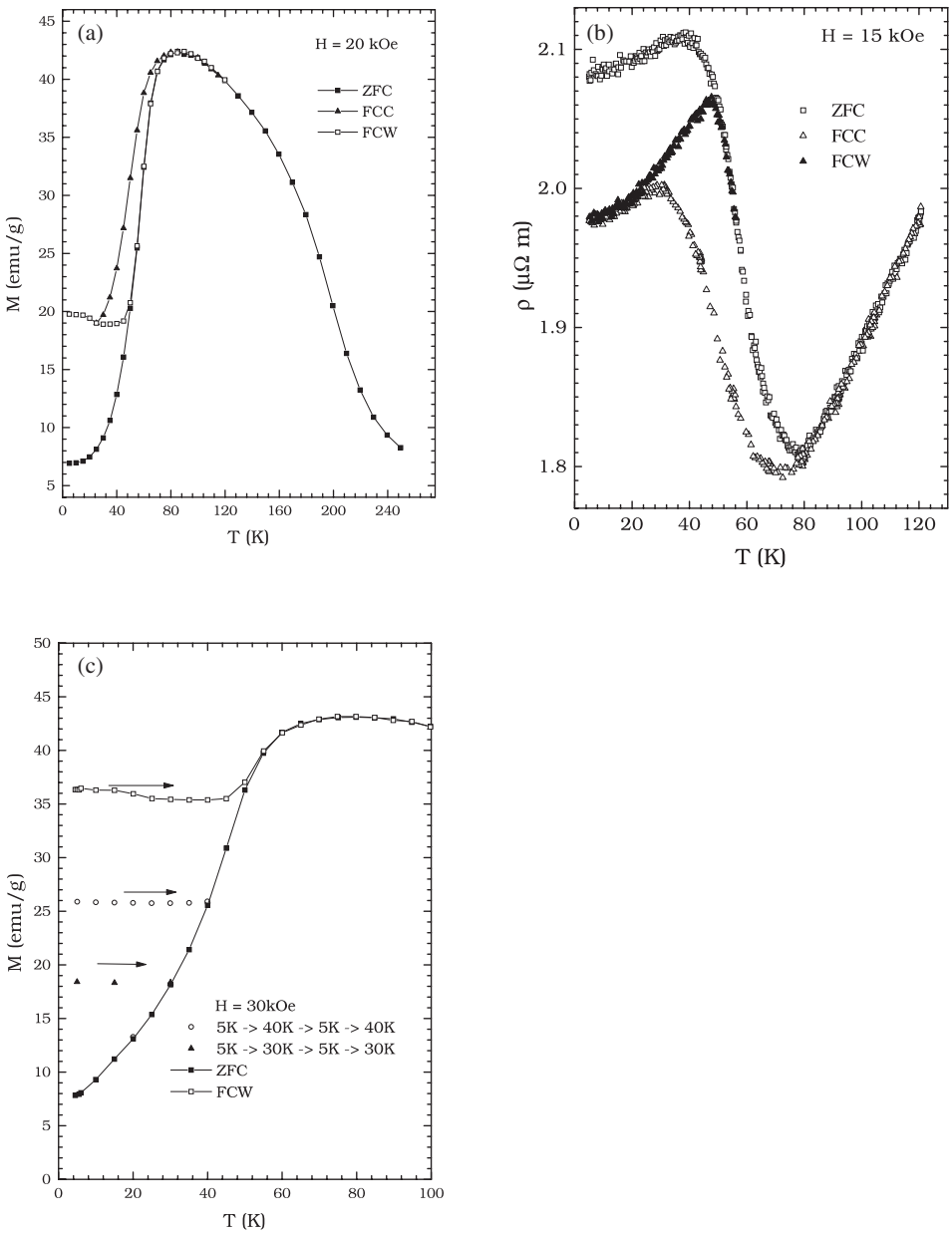

Figure 6. (*a*) Magnetization versus temperature plots in ZFC, FCC and FCW modes at $H = 20$ kOe. (*b*) Resistivity versus temperature in ZFC, FCC and FCW modes at $H = 15$ kOe (see [28]). (*c*) The magnetization versus temperature plot, reversing the direction of temperature change before completing the transition in a field of 30 kOe. The ZFC curve (solid squares), cooling from the ZFC curve at $T = 30$ K down to 5 K and warming back to $T = 30$ K (solid upward-pointing triangles), cooling from the ZFC curve at $T = 40$ K down to 5 K and warming back to $T = 40$ K (open circles). The FC curve is shown by open squares. See the text for details.

temperature limit of metastability T^* [33]. Between T_N and T^*, fluctuations will help in the formation of droplets of the stable AFM state, and at T^* an infinitesimal fluctuation will drive the whole system to a stable AFM state. While lowering T towards T^*, the amount of FM

phase will go on reducing and hence give a decrease in the magnetization. One thus expects the FC magnetization to decrease monotonically with decrease in temperature and merge with the ZFC magnetization (i.e. a complete transformation from a FM to an AFM state). Our results, on the contrary, show that the FC curve is non-monotonic and does not merge with the ZFC curve.

One possibility is that though the size of FM droplets is decreasing with the decrease in temperature, the spins within each of these droplets are getting aligned. These two competing processes can give rise to the observed non-monotonic behaviour of the M–T curve in the FC case. The TMI increasing with increasing field indicates that the separation between the $T_N(H)$ and $T^*(H)$ lines increases as the field is increased and probably we are not able to cool below $T^*(H)$ to get back the AFM phase. This picture however does not explain the virgin M–H and ρ–H curves lying outside the envelope curve. Such a relation between the virgin curve and the envelope curve will arise when a finite amount of FM phase remains even when the field is reduced to zero. This FM phase is then carried over when the direction of field is changed and gives a higher value of magnetization than the virgin curve.

These results (that we are unable to get back the AFM phase completely in both the temperature- and field-induced transitions) indicate that the kinetics of the transition are arrested below a certain temperature. It is possible that the kinetics of the transition slow down just like in the case of the transition from supercooled liquid to glass, where the characteristic time for structural relaxation becomes larger than experimental timescales [34]. Similarly the supercooled FM phase in our case can remain frozen within the experimental time [35]. In this picture the field and temperature regime in which this freezing of supercooled FM phase occurs is such that both the anomalous TMI and the virgin curve lying outside the envelope M–H and ρ–H curves can be explained [35].

Further support for our conjecture of the kinetics of transition getting arrested comes from an experiment whose results for one representative case are shown in figure7. In this experiment a point in the H–T plane (7 kOe, 5 K) is approached by three different paths, namely

(i) in the ZFC mode;
(ii) in the FC mode; and
(iii) by first field cooling the sample in a field higher (40 kOe) than the target field (7 kOe) and then reaching the target field isothermally at 5 K.

After this particular point in the H–T plane is approached, the sample is warmed and the magnetization is measured.

In case (iii) the sample has a magnetization corresponding to point 1 (see figure 7) when field cooled in 40 kOe. Now when the field is reduced to 7 kOe (point 2 in figure 7), the magnetization does not coincide with the field-cooled magnetization at 7 kOe. This behaviour clearly shows that a larger amount of FM phase remains frozen when the sample is cooled in higher fields. If there was no kinetic arrest of the transition, the magnetization at 5 K in case (iii) (after reaching $H = 7$ kOe) should have merged with the 7 kOe field-cooled magnetization at 5 K as is expected from the normal behaviour across a first-order transition. The sample now needs to be warmed to get rid of the kinetically arrested FM fraction. In agreement with this explanation, the magnetization merges with that of the 7 kOe field-cooled case at around $T = 25$ K.

The features that we have observed in our M–T and M–H experiments which can be used to identify a first-order transition with both the temperature and field as control variables are

(i) that the TMI increases with increase in the applied field which is contrary to the case for the TMI observed in the case of spin glasses or hard ferromagnets; and
(ii) the M–H *butterfly loop*, whose counterpart in the case of ferroelectrics is taken to be evidence of a first-order transition.

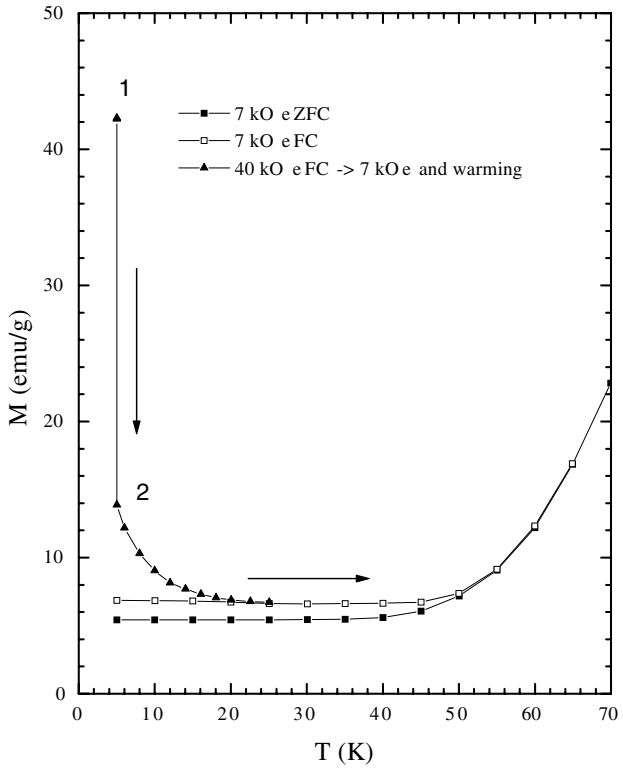

Figure 7. Magnetization versus temperature (during warming) in three different temperature–field histories. (i) The ZFC mode (filled squares). (ii) The FC mode (open squares). (iii) Field cooling the sample in 40 kOe down to 5 K and isothermally reducing the field to 7 kOe (filled upward-pointing triangles). See the text for details.

The non-linearity in the low-field M–H curves and our results that in certain field and temperature regimes we do not get back the AFM state completely after the first field or temperature cycling can raise doubts over the presence of FM impurities. Our magneto-transport study on the same sample negates this possibility. A detailed study of those measurements is presented elsewhere [28].

3.5. Non-linear low-field magnetization

As we pointed out during the discussion on the M–H curve, the low-field magnetic response of the low-temperature (supposedly) AFM state is quite non-linear in nature (see figures 8(*a*) and (*b*)). This behaviour definitely points to the presence of some FM correlation in this low-temperature phase. While it was pointed out earlier that such behaviour probably arose due to an impurity FM phase [10], an intrinsic origin of such behaviour cannot be ruled out entirely [17, 21]. Such non-linearity has been seen in Co-doped [17], Ru-doped [21] and Ir- and Re-doped $CeFe_2$ samples [10]. To address this issue in some more detail, we present in figure 8(*a*) a low-field ($0 \leqslant H \leqslant 5$ kOe) M–H curve for the $Ce(Fe_{0.96}Al_{0.04})_2$ sample obtained in the temperature regime ($5\ \text{K} \leqslant T \leqslant 70$ K). Perceptible non-linearity in the M–H curve is also observed in the temperature regime above T_C ($\approx$200 K) (see figure 8(*b*)). Such behaviour can be attributed to the short-range magnetic interaction, which is observed in the

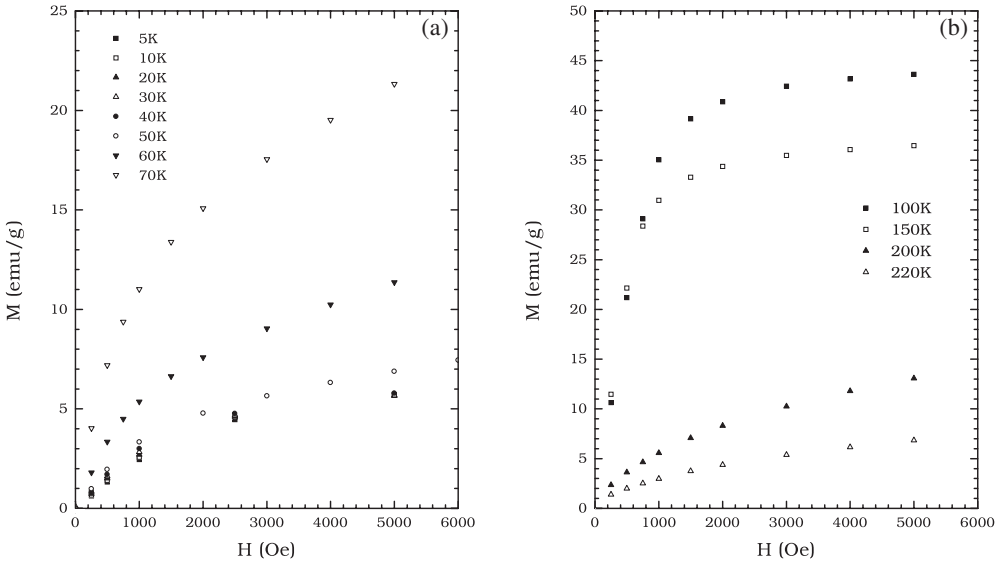

Figure 8. (*a*) Low-field M–H curves for $Ce(Fe_{0.96}Al_{0.04})_2$ for 5 K $\leqslant T \leqslant$ 70 K. See the text for details. (*b*) Comparison of M–H curves in the FM region (T = 100, 150 K) and PM region (T = 200, 220 K).

parent compound $CeFe_2$ even in the temperature regime up to $4T_C$ [36]. The non-linearity and the tendency towards saturation are very prominent in the FM phase and become stronger with the decrease in temperature. This trend persists for $T \approx 100$ K. Below this temperature the AFM phase sets in. It should be noted here that although the non-linearity persists distinctly even in the proposed low-temperature AFM phase, both the initial slope and the actual value of the magnetization decrease with the decrease in T (see figure 8(*a*)). It is also to be noted that both the non-linearity and the value of the magnetization measured at T = 40, 30, 20, 10 and 5 K are less than those observed in the PM regime (at T = 220 K) (see figure 8(*b*)). We have observed very similar behaviour in the Ru- and Ir-doped $CeFe_2$ systems [20]. The suspected FM impurity phase (if any) in the present samples has to be either Ce_2Fe_{17} or pure Fe, but the Curie temperatures of both of these materials are above 250 K. It is now quite clear that the non-linear magnetic behaviour (just described above) of the low-temperature AFM state cannot be explained in terms of these impurity phases in any simple manner. The contribution to the magnetization from the FM impurity phase will either increase or saturate with the decrease in temperature. It is quite likely that some residual intrinsic FM correlations with decreasing strength (with the decrease in temperature) survive in the low-temperature AFM state. This is to be contrasted with the presence of AFM fluctuations in the low-temperature FM state of the parent compound $CeFe_2$ [3]. Careful microscopic measurements (such as neutron diffraction and/or Mössbauer measurements) are now necessary to resolve this problem of the $CeFe_2$-based pseudobinaries.

4. Conclusions

Summarizing our results we can say that, in continuation of our earlier work on Ru- and Ir-doped $CeFe_2$ samples, we have shown here that the transition from antiferromagnetism to ferromagnetism in $Ce(Fe_{0.96}Al_{0.04})_2$ in the presence of a field is also first order in nature.

We have found additional features, namely (i) ZFC/FC irreversibility increasing in degree with increase in the applied field and (ii) the virgin M–H and ρ–H curves lying outside the envelope curve. These anomalous results show clearly that the FM-to-AFM transition kinetics seem to be arrested in the low-temperature and high-field regime.

References

[1] Buschow K H J 1980 *Ferromagnetic Materials* vol 1, ed E P Wohlfarth (Amsterdam: North-Holland)
[2] Eriksson O, Nordstrom L, Brooks M S S and Johansson B 1988 *Phys. Rev. Lett.* **60** 2523
[3] Paolasini L, Dervenagas P, Vulliet P, Sanchez J P, Lander G P, Hiess A, Panchula A and Canfield P 1998 *Phys. Rev.* B **58** 12 117
[4] Franceschini D F and Da Cunha S F 1985 *J. Magn. Magn. Mater.* **52** 280
[5] Rastogi A K and Murani A P 1987 *Theoretical and Experimental Aspects of Valence Fluctuations and Heavy Fermions* ed L C Gupta and S K Malik (New York: Plenum) p 437
[6] Roy S B and Coles B R 1989 *J. Phys.: Condens. Matter* **1** 419
[7] Roy S B and Coles B R 1989 *Phys. Rev.* B **39** 9360
[8] Rastogi A K, Hilscher G, Gratz E and Pillmayr N 1988 *J. Physique Coll.* **49** C8 277
[9] Roy S B, Kennedy S J and Coles B R 1988 *J. Physique Coll.* **49** C8 271
[10] Rajarajan A K, Roy S B and Chaddah P 1997 *Phys. Rev.* B **56** 7808
[11] Kennedy S J, Brown P J and Coles B R 1993 *J. Phys.: Condens. Matter* **5** 5169
[12] Giorgetti C *et al* 1993 *Phys. Rev.* B **48** 12 732
[13] Schille J Ph, Bertan F, Finnazi M, Brouder Ch, Kappler J P and Krill G 1994 *Phys. Rev.* B **50** 2985
[14] Delobbe A, Dias A M, Finnazi M, Stichauer L, Kappler J P and Krill G 1998 *Europhys. Lett.* **43** 320
[15] Cooper M J, Lawson P K, Dixon M A G, Zukowski E, Timms D N, Itoh F, Sakurai H, Kawata H, Tanaka Y and Ito M 1996 *Phys. Rev.* B **54** 4068
[16] Fukuda H, Fujii H, Kamura H, Hasegawa Y, Ekino T, Kikugawa N, Suzuki T and Fujita T 2001 *Phys. Rev.* B **63** 054405
[17] Wada H, Nishigori M and Shiga M 1993 *J. Phys. Soc. Japan* **62** 1337
[18] Ali N and Zhang X 1992 *J. Phys.: Condens. Matter* **4** L351
[19] Kennedy S J and Coles B R 1990 *J. Phys.: Condens. Matter* **2** 1213
[20] Manekar M *et al* 2000 *J. Phys.: Condens. Matter* **12** L409
Manekar M *et al* 2000 *J. Phys.: Condens. Matter* **12** 9645
[21] Kunkel H P, Zhou X Z, Stampe P A, Cowen J A and Williams G 1996 *Phys. Rev.* B **53** 15 099
[22] Chikazumi S 1997 *Physics of Ferromagnetism* (Oxford: Clarendon)
[23] Bean C P and Rodell D S 1962 *Phys. Rev.* **126** 104
[24] Campbell A J, Paul D M K and McIntyre G J 2000 *Phys. Rev.* B **61** 5872
[25] Dekkar A J 1985 *Solid State Physics* (New Delhi: Macmillan India)
[26] Zysler R D *et al* 2000 *J. Magn. Magn. Mater.* **221** 37
Tronc E *et al* 2000 *J. Magn. Magn. Mater.* **221** 63
[27] Bozorth R M 1994 *Ferromagnetism* (Piscataway, NJ: IEEE)
[28] Singh K J *et al* 2002 *Phys. Rev.* B **65** 094419
[29] Mydosh A J 1993 *Spin Glasses: an Experimental Introduction* (London: Taylor and Francis)
[30] Merches M, Shankar S G and Wallace W E 1978 *J. Appl. Phys.* **49** 2055
Roy S B *et al* 1996 *Solid State Commun.* **99** 563
Sun Z *et al* 1999 *J. Appl. Phys.* **86** 5152
Joy P A and Date S K 2000 *J. Magn. Magn. Mater.* **220** 106
[31] Müller M A, Takashige M and Bednorz J G 1987 *Phys. Rev. Lett.* **58** 1143
[32] Roy S B *et al* 1997 *Phil. Mag.* B **75** 303
[33] Chaikin P M and Lubensky T C 1995 *Principles of Condensed Matter Physics* (Cambridge: Cambridge University Press)
[34] Debenedetti P G 1996 *Metastable Liquids* (Princeton, NJ: Princeton University Press) ch 4
[35] Manekar M A *et al* 2001 *Phys. Rev.* B **64** 104416
[36] Deportes J, Givord D and Ziebeck K R A 1981 *J. Appl. Phys.* **52** 2074